

LETTERS

Partial penetrance facilitates developmental evolution in bacteria

Avigdor Eldar^{1*}, Vasant K. Chary^{2*}, Panagiotis Xenopoulos², Michelle E. Fontes¹, Oliver C. Losón¹, Jonathan Dworkin³, Patrick J. Piggot² & Michael B. Elowitz¹

Development normally occurs similarly in all individuals within an isogenic population, but mutations often affect the fates of individual organisms differently^{1–4}. This phenomenon, known as partial penetrance, has been observed in diverse developmental systems. However, it remains unclear how the underlying genetic network specifies the set of possible alternative fates and how the relative frequencies of these fates evolve^{5–8}. Here we identify a stochastic cell fate determination process that operates in *Bacillus subtilis* sporulation mutants and show how it allows genetic control of the penetrance of multiple fates. Mutations in an intercompartmental signalling process generate a set of discrete alternative fates not observed in wild-type cells, including rare formation of two viable ‘twin’ spores, rather than one within a single cell. By genetically modulating chromosome replication and septation, we can systematically tune the penetrance of each mutant fate. Furthermore, signalling and replication perturbations synergize to significantly increase the penetrance of twin sporulation. These results suggest a potential pathway for developmental evolution between monosporulation and twin sporulation through states of intermediate twin penetrance. Furthermore, time-lapse microscopy of twin sporulation in wild-type *Clostridium oceanicum* shows a strong resemblance to twin sporulation in these *B. subtilis* mutants^{9,10}. Together the results suggest that noise can facilitate developmental evolution by

enabling the initial expression of discrete morphological traits at low penetrance, and allowing their stabilization by gradual adjustment of genetic parameters.

Under nutrient-limited conditions, an individual *B. subtilis* cell can develop into a resilient dormant spore¹¹. Many sporulation mutations reduce the fraction of cells that sporulate successfully (Fig. 1a, b)^{4,12–14}. This makes sporulation an ideal model system in which to study the origins and impact of partial penetrance.

At the onset of sporulation, *B. subtilis* cells divide asymmetrically into smaller (forespore) and larger (mother-cell) compartments. Septation leads to the forespore-specific activation of the transcriptional regulator σ^F (Fig. 1c, d)¹¹. This in turn activates expression of *spoIIR*, which initiates an intercompartmental signalling cascade that activates the mother-cell-specific regulator σ^E , causing mother-cell differentiation^{11,15}. Deleting σ^E allows a second asymmetric septum to form, resulting in ‘abortively disporic’ cells with two DNA-containing immature forespores and a mother cell devoid of DNA^{16,17}. Attenuation of *spoIIR* expression results in a partially penetrant mixture of successfully sporulating and abortively disporic cells^{12,13}.

To explore the effects of *spoIIR* mutations on sporulation penetrance, we constructed a set of strains, collectively denoted as *spoIIR*^{PP} mutants, in which the rate and/or the time of onset of *spoIIR* expression is specifically perturbed (Supplementary Methods

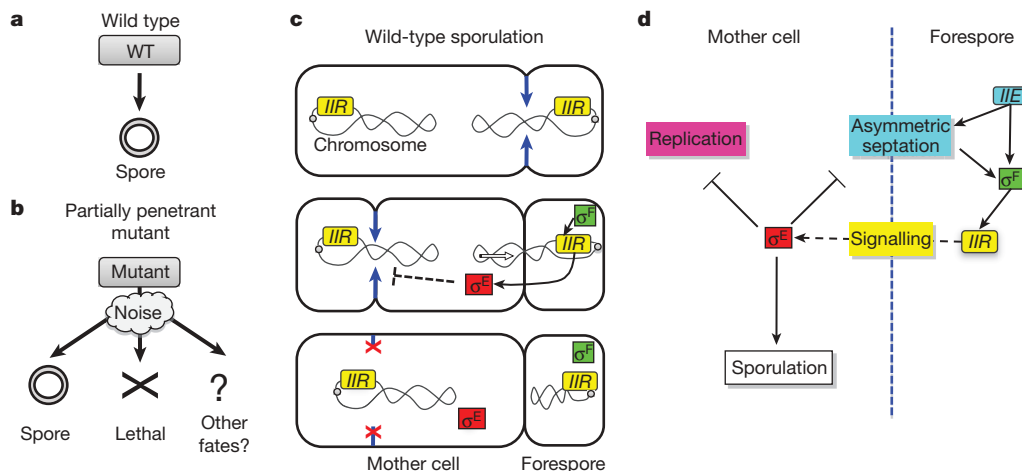


Figure 1 | Partial penetrance in the developmental process of sporulation. **a**, In wild-type sporulation, each sporulating cell produces a single spore. **b**, Partly penetrant mutants exhibit a mixture of normal sporulation, lethal

failures (cross) and alternative viable fates (?) due to cellular fluctuations (cloud). **c, d**, Events (**c**) and genetic interactions (**d**) leading to differentiation of the mother-cell and forespore compartments (see text).

¹Howard Hughes Medical Institute and Division of Biology and Department of Applied Physics, California Institute of Technology, Pasadena, California 91125, USA. ²Department of Microbiology and Immunology, Temple University School of Medicine, 3400 North Broad Street, Philadelphia, Pennsylvania 19140, USA. ³Department of Microbiology, College of Physicians and Surgeons, Columbia University, New York, New York 10032, USA.

*These authors contributed equally to this work.

and Supplementary Figs 1–4). We characterized *spoIIR*^{PP} mutants using time-lapse imaging of cells expressing fluorescent reporters of σ^F and σ^E activity (Methods, Supplementary Fig. 1 and Supplementary Movie 1). These movies revealed a diverse set of discrete cell fates (Fig. 2), whose relative frequencies depended on the type and severity of the perturbation to *spoIIR* expression. In all of these mutants, after an initial asymmetric septation and activation of σ^F in the forespore, mother cells exhibited one of three ‘primary’ fates (Fig. 2a–c). One population of cells activated σ^E and continued to sporulate normally (Fig. 2a). Another population formed the abortively dispore morphology (Fig. 2b). In the third population, neither σ^E activation nor asymmetric septation was observed (Supplementary Fig. 5). In these cells, the activated forespores did not develop further, but the mother cells continued to grow in a process we term ‘sporulation escape’ (Fig. 2c, Supplementary Fig. 5 and Methods)^{11,18}.

Escape enabled the formation of an additional cell type. About 25% of the time, escaping cells immediately re-initiated sporulation. In ~5% of such cases, two new forespores developed sequentially (~20 min apart) within the same mother cell (Fig. 2d and Supplementary Fig. 6). Unlike abortively dispore cells, these ‘twin’ sporulating cells completed sporulation, producing two mature viable spores in a single mother-cell compartment (Supplementary Fig. 7). Twins exhibited the transcriptional and morphological hallmarks of proper sporulation (Fig. 2d and Supplementary Fig. 8). Twin spores germinated properly, and were ultraviolet-resistant (Supplementary Fig. 9). Similar morphologies (called ‘bipolar’) appear to have evolved independently many times in the class Clostridia^{9,10}, the sporulation pathway of which is homologous to that of *Bacillus*¹⁹, but have not been observed in *Bacillus* itself (Supplementary Fig. 10). Twin sporulation may be adaptive under some conditions, including when vegetative growth is inhibited and proliferation occurs principally by sporulation^{10,20}.

The ability of cells to form twins is surprising because only two chromosome copies are present during normal sporulation¹¹, and twins require at least three. Therefore, we tracked the number and cellular compartment of chromosomes tagged with TetR–green fluorescent protein (GFP) ‘dots’ bound to a cassette of chromosomally integrated *tetO* operators (Fig. 2e and Supplementary Fig. 11)^{21,22}. We found that 30% of ‘escaping’ *spoIIR* mutant cells over-replicated to produce three or more chromosomal dots within a single cell. Fifteen per cent of these cells then underwent two consecutive asymmetric septation events without additional replication, producing twins. Because *spoIIR*^{PP} mutations cannot affect chromosome number before the initial septation event (when *spoIIR* is first expressed), this result explains why twins only formed as secondary fates in *spoIIR*^{PP} mutants. Furthermore, some of these over-replicating (polyploid) cells sporulated normally (to produce a single spore), despite the presence of extra chromosomal copies in the mother cell (Fig. 2f and Supplementary Fig. 11).

What determines the fate of an individual cell within a clonal mutant population? Because *spoIIR* mutations have alternative fates, and because sporulation penetrance is directly linked to the strength of *spoIIR* mutations^{12,13} (Supplementary Figs 3 and 4), fluctuations in *spoIIR* expression represent the most direct candidate for fate determination. To test this hypothesis, we constructed a specific *spoIIR*^{PP} strain, called *spoIIR*^{PP-CY} (Supplementary Fig. 2), in which *spoIIR* expression is reduced and delayed by ~10 min, and can be monitored using a co-transcribed *yfp* reporter. The onset of *spoIIR* expression can be compared in the same cell with that of another, non-delayed, σ^F -dependent promoter controlling *cfp* expression (Fig. 3a and Supplementary Fig. 2). We observed variation of 5 min in the timing and ~56% in the rate of *spoIIR* expression ($n = 148$ cells; Fig. 3b, inset). However, *spoIIR* expression rate fluctuations explained only ~15% of the decision between sporulation and other fates (based on relative

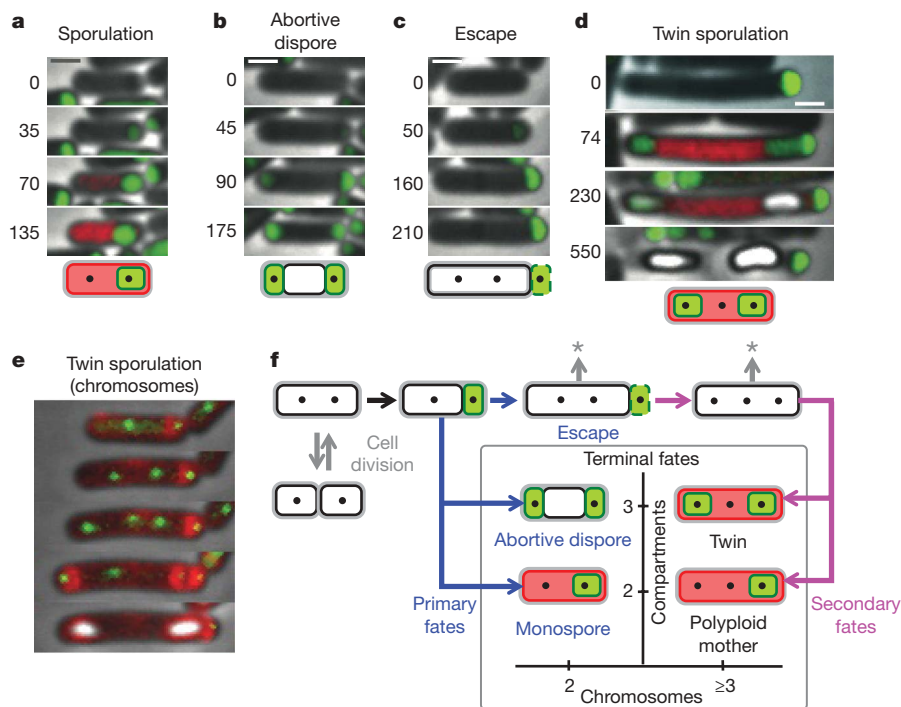


Figure 2 | Time-lapse movies reveal alternative developmental pathways in *spoIIR*^{PP} signalling mutants. **a–d**, Green and red represent fluorescent-protein expression from σ^F - and σ^E -dependent promoters, respectively, overlaid on phase-contrast images (grey). Developing forespores appear white at late times. Times are indicated in minutes from σ^F activation. **a**, Normal sporulation. **b**, Abortively dispore cells. **c**, Escaping cells activate σ^F but continue to elongate without activating σ^E (Supplementary Fig. 5). Note that the activated forespore (right) does not develop further. **d**, Twin sporulation occurs after escape. Green fluorescence at the initial time is a

remnant of escape from the previous sporulation attempt. **e**, Chromosome over-replication occurs before the formation of twin forespores. TetR–GFP-tagged chromosomal loci appear as green dots. Membrane staining (red) shows septation events. The rightmost dot is the remnant from a previous escape. **f**, Temporal sequence of events leading to observed terminal fates, which are classified by the numbers of chromosomes (x axis) and compartments (y axis). An asterisk indicates potential for return to vegetative division and/or additional sporulation attempt. Scale bar, 1 μm .

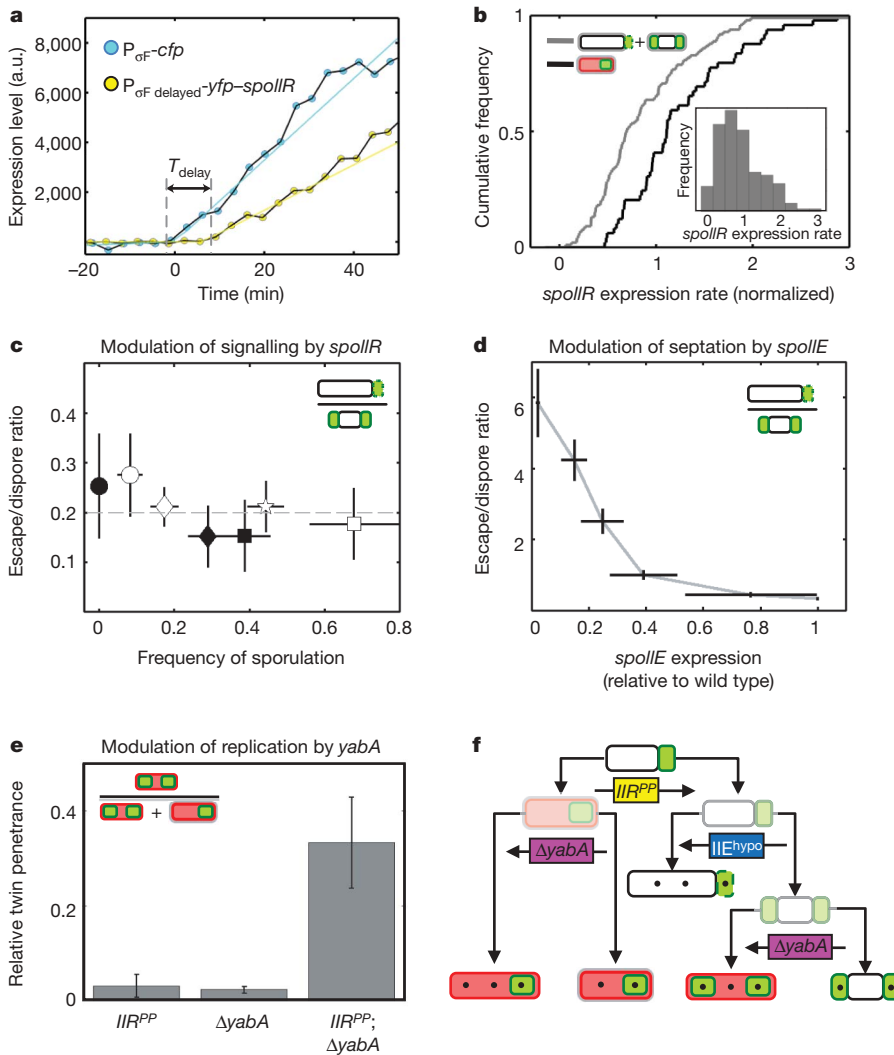


Figure 3 | Noise and gene expression control cell fate in a hierarchical fashion. **a**, Time traces indicating delay (T_{delay} , arrow) and reduction (slope of yellow line compared with that of cyan line) in *spoIIR* expression rate of a typical *spoIIR*^{PP-CY} cell. $P_{\sigma F}$, σ^F -responsive promoter (Supplementary Methods); a.u., arbitrary units. **b**, Cumulative histograms of *spoIIR* expression rate are shown for two subpopulations of a single *spoIIR*^{PP} strain in the same microcolony ($n = 150$ cells). Sporulating cells show a systematically higher level of *spoIIR* expression. Inset, cell–cell variability in *spoIIR* expression rate. **c–e**, Systematic genetic manipulation of fate penetrance. Error bars (s.e.) are based on three replicate experiments. **c**, *spoIIR* expression controls the overall frequency of sporulation (x axis) but does not systematically affect the ratio of escape cells and abortive dispore cells (y axis). Points represent *spoIIR*^{PP} strains differing in *spoIIR* expression level and delay. Symbols correspond to different *spoIIR*^{PP} mutant strains, as defined in Supplementary Methods. Dashed line indicates the mean escape/dispore ratio across the measured strains. **d**, *spoIIE* expression level tunes the penetrance ratio of escape and abortively dispore fates (Methods and Supplementary Fig. 12). **e**, Deletion of *yabA* interacts synergistically with *spoIIR*^{PP} mutants to increase twin penetrance (see also Supplementary Fig. 11). **f**, Fate determination can be controlled hierarchically: different genes affect different decision points.

mutual information; $P < 10^{-4}$). Variation in the expression delay had weaker explanatory power. Thus, fluctuations directly related to the genetic perturbation in *spoIIR* only partially account for cell fate. Much of the fate decision is apparently determined by other fluctuations, whose effects are revealed when *spoIIR* expression is attenuated.

Next we analysed the genetic control of fate penetrance in the *spoIIR*^{PP} mutants. Sporulation frequency varied from 0% in a Δ *spoIIR* mutant to approximately 75% across the set of *spoIIR*^{PP} strains. Strikingly, however, the ratio of escape and abortively dispore frequencies remained approximately constant across this range (Fig. 3c and Supplementary Methods). This behaviour suggests that two independent levels of primary cell fate determination can be distinguished: the decision between sporulating and non-sporulating fates depends on how *spoIIR* is perturbed, whereas the decision between escape and abortively dispore fates is independent of this perturbation (Fig. 3f).

Escape and abortively dispore fates differ in the number of asymmetric divisions they undergo and their ratio therefore may be affected by regulators of asymmetric division. The membrane protein SpoIIE promotes asymmetric septum formation²³, and therefore could have such an effect (Fig. 1d). To test this hypothesis, we constructed a strain, *spoIIE*^{hypo}, in which the level of *spoIIE* expression could be modulated by the inducer isopropyl β -D-1-thiogalactopyranoside (IPTG) without affecting its temporal dynamics (Methods and Supplementary Fig. 12). This strain included a Δ *spoIIR* mutation to make the measurement independent of the additional indirect function of SpoIIE in *spoIIR* activation¹¹ (Fig. 1d). As expected, the ratio of

escape and abortively dispore frequencies increased as the level of *spoIIE* expression was reduced (Fig. 3d and Supplementary Fig. 12).

Similarly, to increase the frequency of twin sporulation would require increasing both the number of chromosomes and the number of compartments generated during sporulation (Fig. 2f). Perturbations of *spoIIR* expression primarily affect compartment number, but have only a modest effect on chromosome number (through the escape state). We reasoned that mutations that increase chromosome copy number could synergize with *spoIIR*^{PP} mutations, increasing the frequency of twins at the expense of abortively dispore cells. To test this possibility, we used two mutations that increase chromosome replication: a null mutation of the chromosome replication inhibitor YabA²⁴ and a hypomorphic fusion of chromosome replication regulator Spo0J with GFP²² (Supplementary Fig. 11). Intriguingly, these over-replication mutations generated a low penetrance of twins in the wild-type background (Fig. 3e), suggesting that they may affect intercompartmental signalling. Combining these mutations with *spoIIR*^{PP} mutants permitted twins, as well as polyploid mother cells, to occur as a primary fate, because some cells then possessed additional chromosomes before the first asymmetric septation event (Supplementary Fig. 11). Finally, the over-replication mutations synergized with signalling mutations, increasing the penetrance of the twin fate to >30% of all viable sporangia, a level comparable to those observed in some natural twin-forming species²⁵ (Fig. 3e and Supplementary Fig. 11). Together, these results indicate, first, that all four terminal fates can be ‘primary’ (that is, occur without a round of escape) and, second, that the penetrance of all fates can

be manipulated by specific genetic perturbations affecting the processes of signalling, septation, and replication (Fig. 3f).

At the evolutionary level, partial penetrance could facilitate transitions between discrete phenotypes by enabling gradual changes in their frequencies, rather than an all-or-none switch from one phenotype to the other, which might require simultaneous changes in multiple processes. As described above, mutations that increase the probability of either additional septation or replication increase the penetrance of the maladaptive abortive-dispore state or the polyloid monospore state, respectively (Figs 2f and 3).

Two conditions would thus facilitate the gradual evolution of twin sporulation. First, a relatively high sporulation efficiency for the polyloid monospore state would allow sequential accumulation of mutations that favour over-replication to be followed by additional mutations that affect septation. We found that polyloid cells carry a fitness cost far smaller than that carried by abortive dispores, completing sporulation successfully about 75% as often as normal sporulating cells (Supplementary Fig. 11). Thus, there does not appear to be any fundamental obstacle to high fitness for this state. Second, mutations that cause correlation between replication and septation would favour the monospore and twin fates over the polyloid and abortive-dispore states. Analysis of fate frequencies revealed evidence for these correlations and their genetic control: in *spoIIR^{PP} spo0J-gfp* mutants, the frequency of reseptation (forming three compartments) differs by a factor of ~ 3 depending on the number of chromosomes observed before asymmetric septation ($P < 10^{-3}$; Fig. 4a). This correlation enhances the penetrance of twins and reduces the penetrance of the maladaptive abortive-dispore state. Neither over-replication nor reseptation is known to occur in wild-type strains; as a result, this correlation may not be under selection, and could therefore vary between backgrounds. Consistent with this, the measured interaction between *spoIIR^{PP}* and *yabA* mutations differed significantly between two closely related strain backgrounds (Fig. 4b). Together, these results suggest that under appropriate selection for twins, *B. subtilis* could acquire mutations that affect septation, replication and their correlation, and thereby enable gradual evolution of twin sporulation.

Finally, we sought to determine whether natural twin sporulation occurs in a manner similar to that observed in *B. subtilis* mutants. We acquired time-lapse movies of *C. oceanicum*, a marine anaerobe that exhibits twin sporulation, with fluorescent-membrane and DNA probes (Supplementary Movie 2)⁹. We observed a partially penetrant mixture of fates including twins and monospores, but not the abortively dispore fate. Analysis of DNA content in monospores was consistent with a subpopulation of polyloid mother cells, as in *B. subtilis* (Supplementary Fig. 13). We analysed the temporal sequence of septation and chromosome replication events in individual cells (Fig. 4c, Supplementary Movie 2 and Methods). DNA staining was observed to increase before the first septation event and

subsequently decrease in the mother cell (Fig. 4e), consistent with replication before the first septation and subsequent translocation of DNA into the forespores, as occurs in *B. subtilis* mutants. The two forespore compartments were formed by consecutive septation events separated by an interval of 30 ± 10 min, slightly longer than observed in *B. subtilis* (Fig. 4d and Supplementary Fig. 6). Together, these results suggest that the natural process of twin development is similar to that observed in the *B. subtilis* mutants.

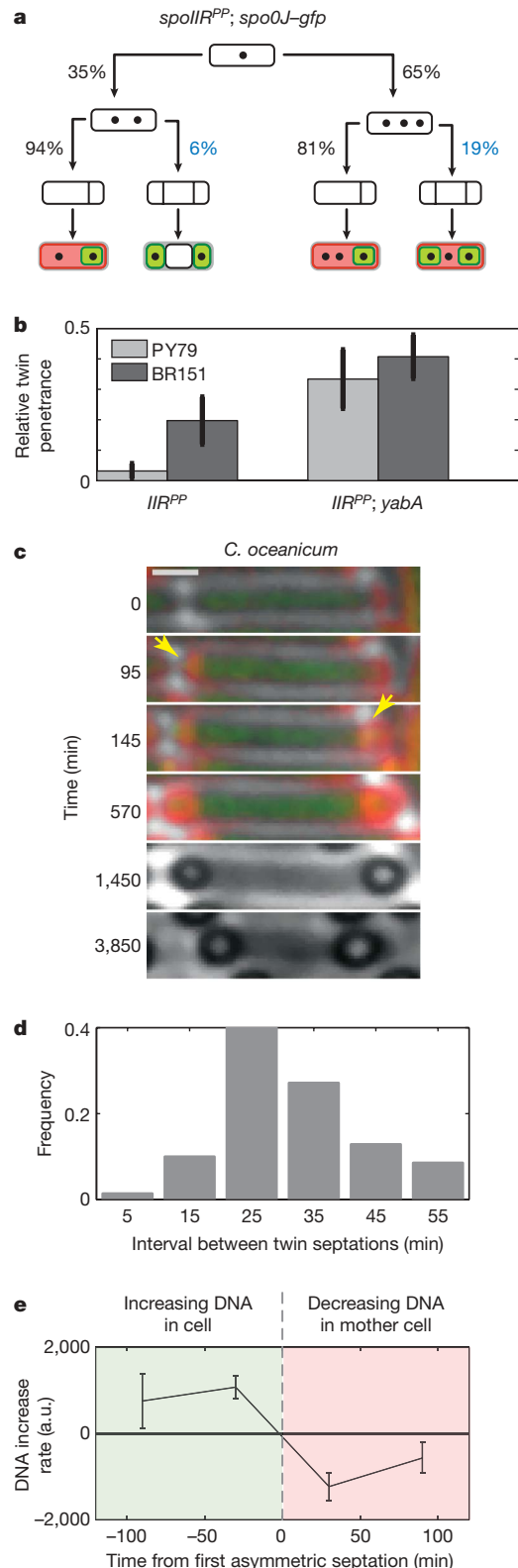


Figure 4 | Evolution of twin sporulation. **a**, Fate tree showing relative frequencies of over-replication (second row) and additional septation (third row) inferred from analysis of terminal fates (bottom row) of $n = 285$ individual cells. Note that the probability of having three compartments depends on chromosome number (blue percentages). Day-to-day variation was $\leq 2\%$ across all measurements. **b**, Strain backgrounds PY79 (used throughout the paper) and BR151 differ in twin penetrance with the same *spoIIR^{PP}* mutation (error bars (s.e.) based on multiple experiments). This difference is reduced by *yabA* mutations. **c–e**, Twin sporulation in *C. oceanicum* resembles that in *B. subtilis* mutants. **c**, Filmstrip showing typical events during *C. oceanicum* sporulation (times in minutes from first frame). Shown are DNA (green), membrane staining (red) and phase contrast (grey). Yellow arrows mark the first appearance of asymmetric septa. **d**, The distribution of time intervals between two septation events during twin sporulation ($n = 70$). **e**, The rate of change of DNA staining was quantified in individual cells. Staining increases before septation (green area), consistent with chromosome replication, and decreases after septation (red area), consistent with transport of DNA into forespores. Data were averaged over $n = 30$ cells owing to cell–cell variability (error bars, s.e.m.).

The concept of developmental canalization was introduced to explain the reproducibility of wild-type development and its contrast with developmental variability in mutants^{26,27}. However, it has been difficult to understand how canalization arises at the molecular level in specific genetic networks and, conversely, how its disruption facilitates the evolution of novel developmental programs. In this case, competition among the core processes of septation, replication and signalling is crucial for generating discrete alternative morphologies (Fig. 3f). Mutations that increase the penetrance of twin sporulation and reduce its dependence on noise provide a gradual mechanism for the stabilization of a discrete change in developmental morphology. The ability to combine single-cell, genetic and evolutionary analyses in bacterial developmental systems like *B. subtilis* sporulation may help to identify basic principles underlying the evolution of developmental mechanisms.

METHODS SUMMARY

Strains and conditions. We derived all *B. subtilis* strains, unless otherwise stated, from parental strain PY79 (ref. 28) using standard protocols²⁹. Details of plasmid and strain construction are described in Methods and Supplementary Methods. We performed sporulation in liquid culture using the exhaustion method in modified Schaeffer's sporulation medium¹². *Clostridium oceanicum* strain ATCC 25647 (ref. 9), was obtained from the American Type Culture Collection. **Experimental procedure.** We placed *B. subtilis* cells on agarose pads containing sporulation-inducing resuspension medium. The time-lapse microscopy protocol we used is described in Methods. Exposure times were minimized to prevent photodamage. For membrane staining, we added FM4-64 (Invitrogen) at a concentration of 0.2–1 $\mu\text{g ml}^{-1}$ to the agarose pad before adding cells, or added MitoTracker Green (Invitrogen) at a concentration of 5 $\mu\text{g ml}^{-1}$. Regulated promoters of the strains spoIIR^{hypo} (Supplementary Fig. 2) and spoIIE^{hypo} were controlled by addition of appropriate levels of IPTG to the agarose pad. *Clostridium oceanicum* microscopy was similar except anaerobic conditions were maintained using a custom nitrogen flow chamber. Chromosomes were stained with Vybrant DyeCycle Green (Invitrogen).

Quantitative analysis. Quantitative movie analysis used custom image analysis code in MATLAB 7 (Mathworks), similar to that previously described³⁰. Briefly, we segmented phase contrast or fluorescence images using edge detection to identify individual cells. Segmented cells were tracked semi-automatically from frame to frame on the basis of position and orientation. Fluorescence was defined as the sum of pixel intensities within the area of the cell. When the same structure appeared at both poles of the cell (for example in abortively disporic cells), we calculated fluorescence separately for the two halves of the cell. Fate frequencies were manually scored on the basis of criteria detailed in Methods.

Full Methods and any associated references are available in the online version of the paper at www.nature.com/nature.

Received 6 December 2008; accepted 15 May 2009.

Published online 5 July; corrected 23 July 2009 (see full-text HTML version for details).

- Horvitz, H. R. & Sulston, J. E. Isolation and genetic characterization of cell-lineage mutants of the nematode *Caenorhabditis elegans*. *Genetics* **96**, 435–454 (1980).
- Queitsch, C., Sangster, T. A. & Lindquist, S. Hsp90 as a capacitor of phenotypic variation. *Nature* **417**, 618–624 (2002).
- Sangster, T. A. *et al.* HSP90 affects the expression of genetic variation and developmental stability in quantitative traits. *Proc. Natl Acad. Sci. USA* **105**, 2963–2968 (2008).
- Coote, J. G. Sporulation in *Bacillus subtilis*. Characterization of oligosporogenous mutants and comparison of their phenotypes with those of asporogenous mutants. *J. Gen. Microbiol.* **71**, 1–15 (1972).
- Rutherford, S. L. & Henikoff, S. Quantitative epigenetics. *Nature Genet.* **33**, 6–8 (2003).
- Felix, M. A. & Wagner, A. Robustness and evolution: concepts, insights and challenges from a developmental model system. *Heredity* **100**, 132–140 (2008).
- West-Eberhard, M. J. Developmental plasticity and the origin of species differences. *Proc. Natl Acad. Sci. USA* **102** (suppl. 1), 6543–6549 (2005).
- Kirschner, M. & Gerhart, J. *The Plausibility of Life: Resolving Darwin's Dilemma* 71–108 (Yale Univ. Press, 2005).
- Smith, L. D. *Clostridium oceanicum*, sp. n., a sporeforming anaerobe isolated from marine sediments. *J. Bacteriol.* **103**, 811–813 (1970).

- Angert, E. R. Alternatives to binary fission in bacteria. *Nature Rev. Microbiol.* **3**, 214–224 (2005).
- Hilbert, D. W. & Piggot, P. J. Compartmentalization of gene expression during *Bacillus subtilis* spore formation. *Microbiol. Mol. Biol. Rev.* **68**, 234–262 (2004).
- Khvorova, A., Chary, V. K., Hilbert, D. W. & Piggot, P. J. The chromosomal location of the *Bacillus subtilis* sporulation gene *spoIIR* is important for its function. *J. Bacteriol.* **182**, 4425–4429 (2000).
- Zupancic, M. L., Tran, H. & Hofmeister, A. E. Chromosomal organization governs the timing of cell type-specific gene expression required for spore formation in *Bacillus subtilis*. *Mol. Microbiol.* **39**, 1471–1481 (2001).
- Piggot, P. J. & Coote, J. G. Genetic aspects of bacterial endospore formation. *Bacteriol. Rev.* **40**, 908–962 (1976).
- Karow, M. L., Glaser, P. & Piggot, P. J. Identification of a gene, *spoIIR*, that links the activation of sigma E to the transcriptional activity of sigma F during sporulation in *Bacillus subtilis*. *Proc. Natl Acad. Sci. USA* **92**, 2012–2016 (1995).
- Eichenberger, P., Fawcett, P. & Losick, R. A three-protein inhibitor of polar septation during sporulation in *Bacillus subtilis*. *Mol. Microbiol.* **42**, 1147–1162 (2001).
- Pogliano, J. *et al.* A vital stain for studying membrane dynamics in bacteria: a novel mechanism controlling septation during *Bacillus subtilis* sporulation. *Mol. Microbiol.* **31**, 1149–1159 (1999).
- Dworkin, J. & Losick, R. Developmental commitment in a bacterium. *Cell* **121**, 401–409 (2005).
- Paredes, C. J., Alsaker, K. V. & Papoutsakis, E. T. A comparative genomic view of clostridial sporulation and physiology. *Nature Rev. Microbiol.* **3**, 969–978 (2005).
- Angert, E. R. & Losick, R. M. Propagation by sporulation in the guinea pig symbiont *Metabacterium polyspora*. *Proc. Natl Acad. Sci. USA* **95**, 10218–10223 (1998).
- Dworkin, J. & Losick, R. Does RNA polymerase help drive chromosome segregation in bacteria? *Proc. Natl Acad. Sci. USA* **99**, 14089–14094 (2002).
- Lee, P. S., Lin, D. C., Moriya, S. & Grossman, A. D. Effects of the chromosome partitioning protein SpoOJ (ParB) on oriC positioning and replication initiation in *Bacillus subtilis*. *J. Bacteriol.* **185**, 1326–1337 (2003).
- Ben-Yehuda, S. & Losick, R. Asymmetric cell division in *B. subtilis* involves a spiral-like intermediate of the cytokinetic protein FtsZ. *Cell* **109**, 257–266 (2002).
- Noiro-Gros, M. F. *et al.* Functional dissection of YabA, a negative regulator of DNA replication initiation in *Bacillus subtilis*. *Proc. Natl Acad. Sci. USA* **103**, 2368–2373 (2006).
- Keis, S., Shaheen, R. & Jones, D. T. Emended descriptions of *Clostridium acetobutylicum* and *Clostridium beijerinckii*, and descriptions of *Clostridium saccharoperbutylacetonicum* sp. nov. and *Clostridium saccharobutylicum* sp. nov. *Int. J. Syst. Evol. Microbiol.* **51**, 2095–2103 (2001).
- Waddington, C. H. Canalization of development and the inheritance of acquired characters. *Nature* **150**, 563–565 (1942).
- Rutherford, S., Hirate, Y. & Swalla, B. J. The Hsp90 capacitor, developmental remodeling, and evolution: the robustness of gene networks and the curious evolvability of metamorphosis. *Crit. Rev. Biochem. Mol. Biol.* **42**, 355–372 (2007).
- Youngman, P., Perkins, J. B. & Losick, R. Construction of a cloning site near one end of Tn917 into which foreign DNA may be inserted without affecting transposition in *Bacillus subtilis* or expression of the transposon-borne *erm* gene. *Plasmid* **12**, 1–9 (1984).
- Harwood, C. R. & Cutting, S. M. *Molecular Biological Methods for Bacillus* (Wiley, 1990).
- Rosenfeld, N., Young, J. W., Alon, U., Swain, P. S. & Elowitz, M. B. Gene regulation at the single-cell level. *Science* **307**, 1962–1965 (2005).

Supplementary Information is linked to the online version of the paper at www.nature.com/nature.

Acknowledgements We thank J. Leadbetter and E. Matson for their help with the anaerobic species. We thank R. Losick, A. Grossman, M. Fujita and A. Arkin for strains and advice. We thank R. Kishony, D. Jones, Wolfgang Schwarz, G. Suel, J.-G. Ojalvo, B. Shraiman, J. Levine, J. C. W. Locke, D. Sprinzak, L. Cai and other members of M.B.E. and P.J.P. labs for helpful discussions. Work in the P.J.P.'s lab was supported by Public Health Service Grant GM43577 from the US National Institutes of Health (NIH). Work in M.B.E.'s lab was supported by NIH grants R01GM079771 and P50 GM068763, US National Science Foundation CAREER Award 0644463 and the Packard Foundation. A.E. was supported by the International Human Frontier Science Organization and the European Molecular Biology Organization.

Author Contributions A.E., V.K.C., J.D., P.J.P. and M.B.E. designed the research; A.E., V.K.C., P.X., M.E.F. and O.C.L. performed the experiments; A.E. and V.K.C. analysed the results; and A.E. and M.B.E. wrote the paper.

Author Information Reprints and permissions information is available at www.nature.com/reprints. Correspondence and requests for materials should be addressed to M.B.E. (melowitz@caltech.edu).

METHODS

Construction of LacI-regulated promoters. Briefly, a *lacO* site was added to the *spoIIR*, *spoIIQ* and *spoIIIE* promoter sequences two base pairs downstream of their -10 RNA polymerase binding sites. Expression was measured and compared with the wild-type promoter using an *mCherry* reporter. The normalized mean time course of gene expression from each of these modified promoters was similar to the corresponding wild-type expression profile and independent of IPTG. See Supplementary Figs 3 and 11 and Supplementary Methods for further details.

Time-lapse microscopy. Cells were grown overnight in CH medium²⁹, diluted back in the morning and grown to an optical density at 600 nm (OD₆₀₀) of 0.6 at 37 °C. They were then resuspended in sporulation-inducing resuspension medium²⁹ for 1.5 h. Subsequently they were diluted 1:2 and 1 µl of the resulting suspension was placed on a ~0.5-cm-square agarose pad made of 1.5% low-melting-point agarose in resuspension medium (Sigma). Pads were sealed in a glass-bottom dish (Willco). Typically ~10% of cells will commit to sporulation immediately, and the rest will grow for three or more generations on the pad before sporulating asynchronously. Time-lapse images were acquired using an epifluorescence inverted microscope (Olympus IX81) with an automated stage (ASI) and a sensitive camera (Hamamatsu ORCA ER), all coordinated using custom software³⁰. The temperature was fixed at 37 °C using a temperature-controlled environmental chamber.

Quantitative analysis. Quantitative movie analysis was done using custom image analysis code in MATLAB 7 (Mathworks), similar to that previously described^{30–32}. To reduce segmentation errors and leaking of signal from a strongly expressing cell to a neighbour with low expression, fluorescence images were de-blurred using the iterative Lucy–Richardson method (via the MATLAB function 'deconvlucy'). The resulting expression curves were fit to a piecewise-linear function composed of pre- and post-expression initiation line segments. The results were used to calculate the time of onset of expression (where the two lines meet), the expression level (the difference in slope of the two lines) and other characteristics of the expression profile.

Fate frequencies. To measure the relative frequencies of different primary fates, time-lapse movies were acquired in which sporulation events were marked either by a forespore reporter or by a membrane marker. Sporulating cells were defined as cells that formed a phase-bright spore. Cases in which the forespore failed at a later stage, turning dark again, were also included in the statistics. The majority of sporulating cells continued developing, to produce a mature spore. Abortively disporic cells were defined as cells that formed a second forespore without mother-cell growth. Most escaping cells elongated as described in the text. A small fraction of cells did not continue to grow and eventually lysed. Another small fraction, classified as escape cells, made two septa in a pattern similar to disporic cells but mother-cell growth continued in a manner resembling other escaped cells³³. We defined twins as cells in which two forespores were engulfed in one mother cell and continued to produce two phase-bright bodies. We

included cases in which one or both twin spores failed at a later stage, becoming phase dark again. Notably, a large fraction of twins did manage to form two mature spores. We checked 150–500 cells in each experiment in which frequency was measured.

Comparison between strain background and environment. Strains PY79 and BR151 are both derived from the transformable *B. subtilis* 168 strain, but were maintained in different laboratories for several decades³⁴. PY79 was obtained from R. Losick (Harvard University); BR151 was obtained from F. Young (then at the University of Rochester) and maintained in the Piggot lab. For the liquid assay, cells were inoculated from an overnight culture grown at 37 °C in modified Schaeffer's sporulation medium. We defined T_0 as the time at which exponential growth ended. Cells were observed using phase-contrast microscopy 7, 8 and 9 h after T_0 , and their twin/monospore ratio was defined at the time point, giving the maximum value. Errors reflect day-to-day variation.

***Clostridium oceanicum* general procedures.** Cells were saved as frozen spore suspensions and were inoculated with a heat-kill step to additionally select against sporulation mutants. Cells were grown at 37 °C in BHI medium (BD) with 0.5 g l⁻¹ L-cysteine·HCl, and prepared in anaerobic conditions under nitrogen flow. Typically, cells grew exponentially to an optical density at 600 nm of ~1. They then shifted to a transition state for ~7 h before initiating sporulation.

***Clostridium oceanicum* time-lapse microscopy and analysis.** Preconditioned medium was prepared from cultures at the end of the transition stage. It was then mixed with 1.5% low-melting-point agarose (Sigma) and solidified. We used 2 µg ml⁻¹ FM4-64 (Invitrogen) to stain membranes and 50 nM Vybrant DyeCycle Green (Invitrogen) to stain DNA. Cells from the same stage as the media were then placed on the pad. Cells typically overgrew and areas with a monolayer of cells were followed. All cell and media handling was done in an anaerobic glove box (Coy). Samples were moved in a sealed jar from the anaerobic glove box to the microscope. Spores typically matured after 4 d. The data were analysed for the timing of septum formation (as judged by eye from the FM4-64 channel) and for the rate of change of DNA level. For that purpose, individual cells were manually segmented and tracked. DNA-marker fluorescence was corrected for background and summed over the area of the cell (before septation) or the mother cell (after septation).

31. Suel, G. M., Garcia-Ojalvo, J., Liberman, L. M. & Elowitz, M. B. An excitable gene regulatory circuit induces transient cellular differentiation. *Nature* **440**, 545–550 (2006).
32. Suel, G. M., Kulkarni, R. P., Dworkin, J., Garcia-Ojalvo, J. & Elowitz, M. B. Tunability and noise dependence in differentiation dynamics. *Science* **315**, 1716–1719 (2007).
33. Becker, E. C. & Pogliano, K. Cell-specific SpoIIIE assembly and DNA translocation polarity are dictated by chromosome orientation. *Mol. Microbiol.* **66**, 1066–1079 (2007).
34. Zeigler, D. R. *et al.* The origins of 168, W23, and other *Bacillus subtilis* legacy strains. *J. Bacteriol.* **190**, 6983–6995 (2008).